

A Novel Nonribose Agonist, LUF5834, Engages Residues That Are Distinct from Those of Adenosine-Like Ligands to Activate the Adenosine A_{2A} Receptor

J. Robert Lane,¹ Carmen Klein Herenbrink, Gerard J. P. van Westen,
Jelle A. Spoorendonk, Carsten Hoffmann, and Adriaan P. IJzerman

Division of Medicinal Chemistry, Leiden/Amsterdam Center for Drug Research, Leiden University, Leiden, the Netherlands (J.R.L., C.K.H., G.J.P.v.W., J.A.S., A.P.IJ.); and Department of Pharmacology and Toxicology, University of Würzburg, Würzburg, Germany (C.H.)

Received September 18, 2011; accepted December 21, 2011

ABSTRACT

The recent publication of both the antagonist- and agonist-bound structures of the adenosine A_{2A} receptor have revealed much about how a ligand may bind to a receptor and cause the conformational changes associated with agonist-mediated activation. In particular, the agonist-bound structure revealed key interactions between the ribose group of adenosine-derived agonists and amino acids in the receptor binding pocket that lead to receptor activation. However, agonists without a ribose group also exist, and we wondered whether such compounds occupy the same agonist binding site. Therefore we used a mutagenesis approach in this study to investigate the mode of binding of 2-amino-4-(4-hydroxyphenyl)-6-(1*H*-imidazol-2-ylmethylsulfanyl)pyridine-3,5-dicarbonitrile (LUF5834), a potent partial agonist without a ribose moiety, compared with the adenosine-derived reference agonist 2-[*p*-(2-carboxyethyl)phenyl-ethylamino]-5'-*N*-ethylcarboxamidoad-

enosine (CGS21680). Mutation of the orthosteric residue Phe168 to alanine abrogated the function of both agonists. However, mutation to alanine of residues Thr88 and Ser277 shown by the crystal structures to interact with the ribose group of adenosine-like ligands had no effect on the potency of LUF5834. Furthermore, alanine mutation of Asn253, which makes a hydrogen-bonding interaction with the exocyclic nitrogen of the adenine ring, had minimal effect on LUF5834 affinity but removed agonist activity of this ligand. Mutation of other residues, such as the highly conserved Trp246 or Glu13, had significant deleterious effects on the function of CGS21680 but little effect on LUF5834. In summary, our findings suggest that this class of agonist interacts with distinct residues to activate the receptor compared with classic adenosine derived agonists.

Introduction

Extracellular adenosine has an important physiological role as a signal of metabolic stress and as a modulator of neurotransmitter release. Its effects are predominantly mediated via the interaction with four adenosine receptor (AR)

subtypes (A₁, A_{2A}, A_{2B}, and A₃), members of the G protein-coupled receptor (GPCR) superfamily (Fredholm et al., 2011). There is significant therapeutic potential for both selective antagonists and agonists of the A_{2A} AR (Jacobson and Gao, 2006; Miyamoto et al., 2009). The development of selective A_{2A} AR ligands will surely be aided by the recent publication of both antagonist- and agonist-bound structures of the A_{2A} AR (Jaakola et al., 2008; Lebon et al., 2011; Xu et al., 2011). The antagonist-bound structure revealed that the binding of the antagonist ZM241385 in the A_{2A} receptor was almost perpendicular to that of retinal, timolol, carazolol, and cyanopindolol in the rhodopsin receptor and the β -adrenergic receptors, respectively (Jaakola et al., 2008, 2010). The furan

This work was supported by the Netherlands Organization for Scientific Research [NWO VENI Grant 863.09.018] (to J.R.L.); a Monash University Larkins Fellowship (to J.R.L.); and Tibotec BVBA (to G.J.P.v.W.).

J.R.L. and C.K.H. contributed equally to this work.

¹ Current affiliation: Drug Discovery Biology, Monash Institute of Pharmaceutical Sciences, Monash University, Parkville, Australia.

Article, publication date, and citation information can be found at <http://molpharm.aspetjournals.org>.

<http://dx.doi.org/10.1124/mol.111.075937>.

ABBREVIATIONS: AR, adenosine receptor; GPCR, G protein-coupled receptor; ZM241385, 4-{2-[7-amino-2-(2-furyl)-1,2,4-triazolo[1,5-a][1,3,5]triazin-5-yl-amino]ethyl} phenol; ECL, extracellular loop; LUF5834, 2-amino-4-(4-hydroxyphenyl)-6-(1*H*-imidazol-2-ylmethylsulfanyl)-pyridine-3,5-dicarbonitrile; CGS21680, 2-[*p*-(2-carboxyethyl)phenylethylamino]-5'-*N*-ethyl-carboxamidoadenosine; CFP, cyan fluorescent protein; FIAsh, fluorescein arsenical hairpin binder; PSB-603, 8-[4-[4-(4-chlorophenyl)piperazine-1-sulfonyl]phenyl]-1-propylxanthine; ADA, adenosine deaminase; GPCR, G protein-coupled receptor; BSA, bovine serum albumin; HEK, human embryonic kidney; GFP, green fluorescent protein; TBS, Tris-buffered saline; PDB, Protein Data Bank; MOE, Molecular Operating Environment; ELISA, enzyme-linked immunosorbent assay; UK 432097, 6-(2,2-diphenylethylamino)-9-((2*R*,3*R*,4*S*,5*S*)-5-(ethylcarbamoyl)-3,4-dihydroxytetrahydrofuran-2-yl)-*N*-(2-(3-(1-(pyridin-2-yl)piperidin-4-yl)ureido)ethyl)-9*H*-purine-2-carboxamide; NECA, 5'-*N*-ethylcarboxamidoadenosine; TM, transmembrane.

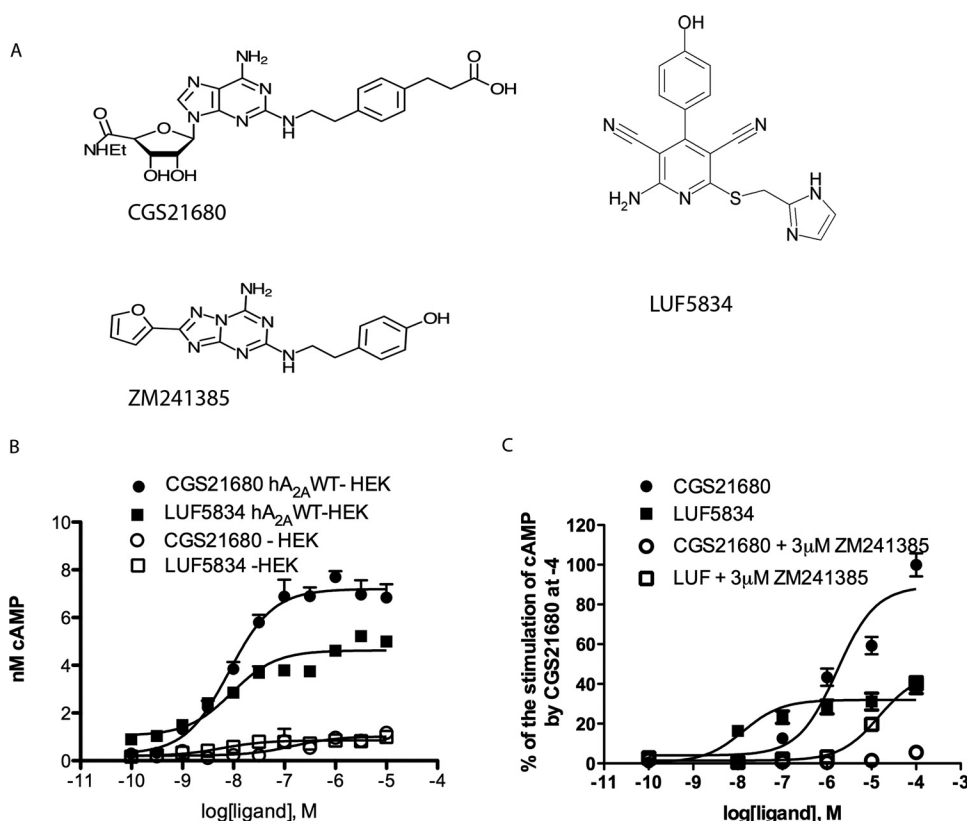


Fig. 1. A, chemical structures of the classic adenosine-like selective A_{2A} AR agonist CGS21680, the novel nonribose agonist LUF5834, and the antagonist ZM241385. B, effects of CGS21680 (circles) or LUF5834 (squares) upon intracellular cAMP production upon HEK293 cells transiently transfected with the adenosine A_{2A} AR (filled shapes) or untransfected HEK293 cells (open shapes). C, the ability of CGS21680 (circles) or LUF5834 (squares) to stimulate intracellular cAMP production in untransfected HEK293 cells is antagonized with a high concentration of the adenosine receptor antagonist ZM241385. Values represent mean \pm S.E.M. from at least three separate experiments.

ring moiety in 4-[2-[7-amino-2-(2-furyl)-1,2,4-triazolo[1,5-*a*][1,3,5]triazin-5-yl-amino]ethyl] phenol (ZM241385; see Fig. 1) was located deep in the binding pocket; the central aromatic triazolo[1,5-*a*]triazine core made a π - π stacking interaction with Phe168^{5,29}, hydrophobic interactions with the Ile274^{7,39} and Leu249^{6,51}, and polar interactions with the highly conserved Asn253^{6,55} and Glu169^{5,30} residues (Jaakola et al., 2008). The 4-hydroxyphenylethyl side chain extended into the extracellular region of the binding cavity. Lebon et al. (2011) and Xu et al. (2011) described the A_{2A} AR cocrystallized with adenosine or adenosine-derived agonists bound. The *adenine core* of such agonists is a common scaffold and is present in nearly all major types of AR agonists and a number of antagonists. This moiety aligns to the heterocyclic core of ZM241385 when the two complex structures are superimposed together, as already predicted in modeling studies (Ivanov et al., 2009; Jaakola et al., 2010). The molecular interactions that anchor ZM241385 in this region are also conserved in the agonist-bound cavity, including aromatic stacking with Phe168 in extracellular loop 2 (ECL2), nonpolar interaction with Ile274^{7,39}, and two hydrogen bonds with Asn253^{6,55} (Lebon et al., 2011; Xu et al., 2011). These structures followed closely behind agonist bound or “active” structures of the β -adrenergic receptors and that of retinal free opsin (Scheerer et al., 2008; Kobilka, 2011; Rasmussen et al., 2011; Rosenbaum et al., 2011; Warne et al., 2011). In all cases, the binding of agonists caused large-scale rearrangement at the cytoplasmic end of the transmembrane helices, including a pronounced inward tilt of helices V and VII and an outward tilt of helix VI, although the degree and direction of movements differ between structures. In contrast the subtle conformational changes within the binding site induced by agonist binding are distinct, suggesting that rather dis-

parate triggers can induce activation of these GPCRs. This leads to the question of whether structurally different orthosteric agonists binding to the same receptor activate the receptor via conserved or distinct interactions. Traditionally, agonists of the adenosine receptors have all been derivatives of the endogenous ligand adenosine. The ribose moiety of such derived compounds was thought necessary for the agonistic behavior of adenosine receptor ligands (Soudijn et al., 2003). In the agonist-bound crystal structure, the ribose moiety of the ligand inserts deeply into a predominantly hydrophilic region of the binding cavity, making hydrogen bonds with His278^{7,43}, Ser277^{7,42}, His250^{6,52}, and Thr88^{3,36} in accord with previous mutagenesis studies (Kim et al., 1995; IJzerman et al., 1996; Jiang et al., 1996; Gao et al., 2000; Kim et al., 2003; Jacobson et al., 2005). Besides these polar interactions, the ribose part of the ligand has close contacts with Val84^{3,32}, Leu85^{3,33}, Trp246^{6,48}, Met177^{5,38}, and Leu249^{6,51}. However, a series of novel ligands for the adenosine receptor that do not contain the ribose moiety have been disclosed in patent literature. These compounds were demonstrated to have both a significant affinity and efficacy toward different adenosine receptor subtypes (Rosentreter et al., 2001, 2003; Beukers et al., 2004; Chang et al., 2005; Heitman et al., 2006). One of these compounds was 2-amino-4-(4-hydroxyphenyl)-6-(1*H*-imidazol-2-ylmethylsulfanyl)-pyridine-3,5-dicarbonitrile (LUF5834), a high-affinity nonadenosine partial agonist at the A_{2A} AR (Beukers et al., 2004).

In this study, we explore the binding mode of this novel agonist using a mutagenesis approach in comparison with the adenosine-derived A_{2A} selective agonist 2-[*p*-(2-carboxyethyl)phenylethylamino]-5'-*N*-ethyl-carboxamido-adenosine (CGS21680) against the background of both the antagonist and agonist bound structures of the A_{2A} AR. These studies

reveal that although these two ligands have an overlapping binding domain, the mutagenesis of several key binding site residues has distinct but often opposite effects upon the potency and efficacy of the two agonists.

Materials and Methods

Materials. The plasmids with the fluorescein arsenical hairpin binder (FAsH)-tagged, CFP-tagged mutated receptors and a cell line that stably expressed the FAsH-tagged, CFP-tagged wild-type receptor were provided by author C.H. 8-[4-[4-(4-Chlorophenyl)piperazine-1-sulfonyl]phenyl]-1-propylxanthine (PSB-603) and cilostamide were obtained from Tocris (Ellisville, MO). 2-[p-(2-Carboxyethyl)phenyl-ethylamino]-5'-N-ethylcarboxamidoadenosine (CGS21680) was a gift from Dr. R. A. Lovell (Ciba-Geigy, Summit, NJ) and rolipram a gift from Dr. N. Sprzagala (Schering AG, Berlin, Germany). 4-[2-[7-Amino-2-(2-furyl)-1,2,4-triazolo[1,5-a][1,3,5]triazin-5-yl-amino]ethyl] phenol (ZM241385) was obtained from AstraZeneca Pharmaceuticals LP (Wilmington, DE) and LUF5834 was made in house. Adenosine deaminase (ADA) was purchased from Roche Diagnostics (Indianapolis, IN), bovine serum albumin (BSA) was obtained from Sigma-Aldrich (St. Louis, MO), and bicinchoninic acid was obtained from Thermo Fisher Scientific (Waltham, MA). All other chemicals were obtained from standard commercial sources.

Cell Culture and Transfection. Human embryonic kidney (HEK) 293 cells were grown as monolayers in Dulbecco's modified Eagle's medium supplemented with stable glutamine, 10% newborn calf serum, streptomycin, and penicillin at 37°C in a moist, 7% CO₂ atmosphere. HEK293 cells stably expressing the wild-type receptor were grown in the same medium as the HEK293 cells but with the addition of G-418 (200 µg/ml). The cells were subcultured by trypsinization. Cells were transfected with plasmid DNA using a calcium phosphate method as described previously (Jaakola et al., 2010). Experiments were performed 48 h after transfection.

cAMP Assay. HEK293 cells were grown and transfected as described above. Experiments were performed 48 h after transfection. Cells were harvested, counted, and resuspended in stimulation buffer and added to 384-well OptiPlates (PerkinElmer Life and Analytical Sciences) at a concentration of 5000 cells/well. The assay was performed following the protocol recommended in the LANCE cAMP 384 kit (PerkinElmer Life and Analytical Sciences) and as described previously (Jaakola et al., 2010). Deviations from the kit protocol are as follows. The stimulation buffer used was phosphate-buffered saline with the addition of 5 mM HEPES, 0.1% BSA, 50 µM rolipram, 50 µM cilostamide, and 0.8 IU/ml ADA. The assay was performed in white 384-well OptiPlates (PerkinElmer Life and Analytical Sciences). Cells were incubated with either CGS21680 or LUF5834 for 45 min at 37°C. After addition of the detection/antibody mix, the plates were left for 3 h at room temperature before reading using a VICTOR² plate reader (PerkinElmer Life and Analytical Sciences). For the mutant receptors E169^{S30A} and N253^{S65A}, concentration-response curves of the agonist CGS21680 were recorded in the presence of increasing concentrations of the antagonist ZM241385 and the partial agonist LUF5834, respectively.

Membrane Preparation. Cells were detached from the plates (10 cm) by scraping into 5 ml of phosphate-buffered saline and centrifuged for 5 min at 1000 rpm. The pellets were resuspended in ice-cold 25 mM Tris-HCl buffer and 5 mM MgCl₂, pH 7.4, and homogenized with an Ultra Turrax homogenizer (IKA-Werke GmbH & Co. KG, Staufen, Germany). Membranes and the cytosolic fraction were separated by centrifugation at 31,000 rpm in an Optima LE-80 K ultracentrifuge (Beckman Coulter, Fullerton, CA) at 4°C for 20 min. The pellets were resuspended in 10 ml of Tris-HCl buffer, and both the homogenization and centrifugation steps were repeated. Tris-HCl buffer was used to resuspend the pellet, and ADA (0.8 IU/ml) was added. The membranes were stored in 250-µl aliquots at -80°C. Membrane protein concentrations were measured using a bicinchoninic acid protein determination.

Radioligand Binding Assays. Binding assays were performed in a 100-µl reaction volume containing 25 mM Tris-HCl buffer, 5 mM MgCl₂, pH 7.4, and 20 µg of membrane protein. The ability of increasing concentrations of the antagonist ZM241385 and agonists CGS21680 and LUF5834 to compete with [³H]ZM241385 (50 Ci/mmol; ARC Inc., St. Louis, MO) for binding to several A_{2A} AR constructs was tested. Nonspecific binding was determined with 1 mM theophylline. Homologous competition binding experiments were carried out using 0.5 nM and 1.0 nM [³H]ZM241385, whereas the displacement assays with CGS21680 and LUF5834 were carried out with 1.7 nM [³H]ZM241385. Incubation was for 2 h at 25°C. Separation of bound from free radioligand was performed by rapid filtration through GF/B filters (Whatman, Clifton, NJ) using an MY-24 harvester (Brandel Inc., Gaithersburg, MD). The filters were washed three times with 50 mM ice-cold Tris-HCl buffer, pH 7.4. Filter bound radioactivity was measured by scintillation spectrometry after the addition of 3.5 ml of Packard Emulsifier Safe using a Tri-Carb 2900TR liquid scintillation analyzer (PerkinElmer Life and Analytical Sciences).

Enzyme-Linked Immunosorbent Assay. Cells were transfected as described under *Cell Culture and Transfection*. Twenty-four hours after transfection, cells were split into 48-well poly-D-lysine-coated plates at a density of 10⁵ cells per well. After an additional 24 h, the cells were fixed with 4% formaldehyde, permeabilized with NP-40, and labeled with anti-green fluorescent protein (GFP) antibody (Living Colors A.V. Peptide Antibody, 1:400; Clontech, Mountain View, CA) in Tris-buffered saline (TBS)/0.1% BSA overnight at 4°C. The following day, the cells were washed with TBS and blocking buffer (0.1 M NaHCO₃ and 1% fat-free milk), and peroxidase-conjugated AffiniPure goat anti-rabbit IgG (1:5000; Jackson ImmunoResearch Laboratories, West Grove, PA) was added as the secondary antibody. The cells were washed three times with TBS. Finally, the cells were incubated with 3,3',5,5'-tetramethylbenzidine liquid substrate system (Sigma) for 3 min in the dark at room temperature. The reaction was stopped with 0.5 M H₂SO₄, and the absorbance was read at 450 nm using a VICTOR² plate reader (PerkinElmer Life and Analytical Sciences).

Docking Studies of LUF5834. Docking was performed in ICM Pro (version 3.6-1h; Molsoft, San Diego, CA) using the crystal structure of the A_{2A} receptor cocrystallized with an agonist deposited in the PDB (code 3QAK). Hydrogens were added to the PDB file by ICM object conversion, which contains hydrogen bond optimization, protonation state optimization of His residues, and rotamer optimization of Asn, Gln, and His residues. All waters were retained in the crystal structure before docking. After removal of the cocrystallized ligand, it was redocked where ICM was able to regenerate the original pose with a root-mean-square deviation of 0.6 Å when calculated for all atoms. Subsequently, both CGS21680 and LUF5834 were docked into the receptor. The binding site was defined by a 7.5-Å sphere around the cocrystallized ligand. Docking itself was performed using the VLS package in ICM with a thoroughness of 2. The top 10 poses were visually inspected. Two dimensional interaction maps were created manually from the docked poses. The docked structures were loaded as PDB files in Molecular Operating Environment (version 2010.10; Chemical Computing Group, Montreal, QC, Canada), and subsequently an interaction map was drawn. However, because the force field in MOE is different from that in ICM Pro, the interactions displayed in MOE show subtle differences from those in ICM Pro. Therefore, the maps from MOE were used as a basis and manually adapted to shown the interactions as they are present in ICM Pro. This included the addition of residues not in direct contact with the ligand (Tyr^{91,35}, Glu^{131,39}, and Ala^{632,61}) to the figure and setting the hydrogen bond energy cutoff at -0.15 kcal/mol.

Data Analysis. The results were analyzed using Prism (version 5.0; GraphPad Software Inc., San Diego, CA). The values are expressed as mean ± S.E.M. of three independent experiments per-

formed in duplicate or triplicate. Agonist concentration response curves were fitted to the following four-parameter Hill equation:

$$\text{response} = \frac{(\text{top} - \text{bottom})}{1 + (10^{\log \text{EC}_{50}/x})^{n_H}} \quad (1)$$

where top represents the maximal asymptote of the concentration response curves, bottom represents the lowest asymptote of the concentration-response curves, $\log \text{EC}_{50}$ represents the logarithm of the agonist EC_{50} , x represents the concentration of the agonist and n_H represents the Hill slope.

To determine a value of affinity for LUF5834, functional data were fitted to an operational model (Black and Leff, 1983) using Prism software according to the equation:

$$\text{Effect} = \frac{\text{Effect}_{\max} \tau [A]}{(K_b + [A]) + \tau [A]} \quad (2)$$

in which K_b is the dissociation constant of agonist binding, Effect_{\max} is the maximum effect with a full agonist, and τ is a measure of agonist efficacy and is defined by the equation

$$\tau = \left(\frac{K_b}{[\text{EC}_{50}]} \right) - 1 \quad (3)$$

It should be noted that for a full agonist $\tau \gg 1$, so $[\text{EC}_{50}]$ approaches K_b/τ .

The pA_2 value is the affinity of antagonists determined by Schild plot analysis using the following equation:

$$\text{pA}_2 = \text{Log}(\text{DR} - 1) - \text{log}[B] \quad (4)$$

where DR is the EC_{50} of the agonist in presence of antagonist divided by the EC_{50} of the agonist in absence of antagonist, and $[B]$ is the concentration antagonist.

The concentrations that inhibited half of the $[^3\text{H}]\text{ZM241385}$ binding (IC_{50}) and the affinities (K_i) of each ligand for the wild-type receptor and T88^{3,36}A and S277^{7,42}A mutated receptors were determined with the use of nonlinear regression analysis and the following equation:

$$Y = \frac{(\text{top} - \text{bottom})x^{n_H}}{x^{n_H} + \text{IC}_{50}^{n_H}} \quad (5)$$

where Y denotes the percentage specific binding, top and bottom denote the maximal and minimal asymptotes, respectively, x denotes the inhibitor potency (midpoint location) parameter, and n_H denotes the Hill slope factor. Assuming simple competition IC_{50} values were converted to K_i values using the Cheng and Prusoff (1973) equation.

Both one- and two-site binding models were tested. The maximum receptor density (B_{\max}) and ligand binding affinity (K_D) were determined with a homologous competition binding assay using the following equation:

$$Y = \frac{B_{\max} \cdot [\text{Hot}]}{[\text{Hot}] + [\text{Cold}] + K_d} + \text{NS} \quad (6)$$

where Y is total ligand binding, $[\text{Cold}]$ is the concentration of unlabeled ligand, $[\text{Hot}]$ is the radioligand concentration, and NS is non-specific binding. Where indicated (Figs. 1, 3, 4, and 6), concentration-effect data are normalized as a percentage, taking the basal response in the control condition as zero and the maximal stimulation of CGS21680 in the control condition as 100%. Statistical analyses were performed with an unpaired t test. Values were stated as significantly different at $P < 0.05$.

Results

Use of Modified A_{2A} AR Constructs with a FIAsh Tag within the Third Intracellular Loop and a C-Terminal CFP Tag. The aim of this project was to investigate the

potential distinct active conformations invoked by two structurally distinct agonists; CGS21680 and LUF5834. The FIAsh-based approach has previously been used to monitor agonist-dependent changes in fluorescence resonance energy transfer signals by measuring those signals between a FIAsh label within the third intracellular loop of the A_{2A} AR and a C-terminal CFP tag (Hoffmann et al., 2005). Consequently, this seemed to be an appropriate technique to attempt to monitor conformational changes caused by binding of the two agonists. However, LUF5834 was too lipophilic for use in our microscopy system. Previously published data showed that this tagged receptor construct had pharmacological features identical to those of the wild-type, among others, in its ability to increase intracellular cAMP levels (Hoffmann et al., 2005). Consequently, we made use of these constructs to pursue a traditional pharmacological approach, and all constructs within this article, including the “wild type” are FIAsh-CFP-tagged receptors.

LUF5834 Is a High-Potency Partial Agonist at the Adenosine A_{2A} AR. The A_{2A} AR is a G_s -coupled GPCR; consequently, an appropriate method to assess receptor activation is to measure increases in intracellular cAMP. In this study, we have made use of the LANCE cAMP 384 assay (PerkinElmer Life and Analytical Sciences). Using HEK293 cells that stably expressed the wild-type A_{2A} AR, the ability of the novel nonribose agonist LUF5834 to stimulate the A_{2A} AR was compared with that of the classic selective adenosine-derived agonist CGS21680 (Fig. 1A). Despite the absence of a ribose pharmacophore within the ligand, LUF5834 was shown to be a partial agonist at the A_{2A} AR with a high potency similar to that of the classic agonist CGS21680 (EC_{50} : LUF5834, 16 nM; CGS21680, 21 nM; Table 1). LUF5834 had an E_{\max} of 41% of the full agonist CGS21680 (Fig. 1B; Table 1). Using an operational model of partial agonism to gain a value of affinity for LUF5834 and assuming CGS21680 to be a full agonist we determined a pK_A of 7.49 ± 0.14 (32 nM) for LUF5834. HEK293 cells are known to endogenously express the A_{2B} AR (Cooper et al., 1997). Given the previously reported high potency of LUF5834 at the A_{2B} AR, it was important to characterize the action of both CGS21680 and LUF5834 on untransfected HEK293 cells before embarking on further mutagenesis studies. CGS21680 is a selective A_{2A} AR agonist with a reported 10,000-fold lower affinity at the A_{2B} AR (Fredholm et al., 2011). Accordingly, CGS21680 caused a dose-dependent increase in cAMP with an EC_{50} value of 10 μM compared with the EC_{50} value of 21 nM observed for the A_{2A} AR expressing HEK293 cells. This signal was completely abolished with the addition of the $\text{A}_{2A}/\text{A}_{2B}$ -selective antagonist ZM241385 (Fig. 1C). This lower potency is in line with an A_{2B} AR-mediated effect. It is noteworthy that this difference in potency is smaller compared with the published values of affinity for CGS21680 at the A_{2A} and A_{2B} ARs. This is surprising given that the A_{2A} AR is overexpressed. However, the efficiency with which the receptor is coupled to the signaling pathway must also be taken into account. A similar phenomenon has been observed for 5HT_{1B} receptors endogenously expressed in Chinese hamster ovary cells (Giles et al., 1996). In this case, the inability to detect receptor expression with radioligand binding indicated a very low level of receptor expression. However, the extremely high potency of agonists, including serotonin and the partial agonist activity of the normally silent antagonist

TABLE 1

CGS21680 and LUF5834 induced stimulation of cAMP mediated by the wild-type and mutant adenosine A_{2A} receptorscAMP production stimulated by CGS21680 and LUF5834 was measured in intact HEK293 cells that stably expressed the wild-type receptor or in transiently transfected cells that expressed the mutant adenosine A_{2A} receptors. The table shows mean \pm S.E.M. calculated from three independent experiments, each performed in triplicate. Change is expressed as the fold increase in the EC₅₀ value for the mutant over that for WT. Efficacy of LUF5834 is expressed as a percentage of CGS21680.

Construct	CGS21680		LUF5834		Efficacy of LUF5834
	pEC ₅₀ (EC ₅₀)	Change	pEC ₅₀ (EC ₅₀)	Change	
	nM	fold	nM	fold	
Wild-type	7.7 \pm 0.1 (21.4)	1.0	7.8 \pm 0.2 (16.2)	1.0	41 \pm 4
E13 ^{1.39} A	6.9 \pm 0.1** (120)	5.6	8.4 \pm 0.1* (4.2)	0.3	28 \pm 4
L85 ^{3.33} A	5.7 \pm 0.1*** (1800)	84	N.D. ^a	N.D. ^a	N.D. ^a
L85 ^{3.33} R	4.9 \pm 0.1*** (13,400)	630	6.4 \pm 0.1** (422.0)	26	43 \pm 4
T88 ^{3.36} A	4.5 \pm 0.0*** (35,900)	1700	7.9 \pm 0.1 (13.6)	0.8	N.D. ^b
F168 ^{5.29} A	4.9 \pm 0.1*** (13,000)	590	5.0 \pm 0.0*** (11,300)	700	34 \pm 9
F168 ^{5.29} D	N.D. ^c	>100,000	N.D. ^c	>100,000	N.D. ^b
E169 ^{5.30} A	7.6 \pm 0.0 (27.2)	1.3	8.3 \pm 0.0* (5.6)	0.4	71 \pm 7*
W246 ^{6.48} A	6.1 \pm 0.0*** (816.0)	38	8.3 \pm 0.0* (5.1)	0.3	30 \pm 4
W246 ^{6.48} Y	8.2 \pm 0.2 (6.6)	0.3	9.7 \pm 0.1*** (0.2)	0.01	42 \pm 4
N253 ^{6.55} A	5.5 \pm 0.1*** (3100)	140	N.D. ^d	N.D. ^d	N.D. ^d
H264 ^{6.66} A	7.1 \pm 0.2* (81.9)	3.8	8.2 \pm 0.0 (6.0)	0.4	57 \pm 5
S277 ^{7.42} A	5.6 \pm 0.1*** (2280)	110	8.2 \pm 0.2 (6.6)	0.4	94 \pm 2***

N.D., not determined.

* $P < 0.05$, significantly different from the wild-type receptor as determined by an unpaired t test.** $P < 0.01$, significantly different from the wild-type receptor as determined by an unpaired t test.*** $P < 0.001$, significantly different from the wild-type receptor as determined by an unpaired t test.^a cAMP levels were too low to determine an accurate EC₅₀ value.^b Potency of CGS21680 was too low to accurately determine the efficacy.^c Potency was too low to determine an accurate EC₅₀ value.^d No stimulation of cAMP was observed up to 100 μ M LUF5834.

cyanopindolol indicated a very efficient coupling of a low density of 5HT_{1B} receptors. It is noteworthy that the levels of intracellular cAMP generated in the untransfected HEK293 were <10% than those observed in the HEK293 cells stably expressing the A_{2A} AR (Fig. 1B). LUF5834 has a high potency at the A_{2B} AR; accordingly, showed a high potency (15 nM) in the untransfected HEK293 cell line. Again, this effect could be antagonized with the addition of ZM241385. The maximal effect exerted by LUF5834 in the untransfected HEK293 cell line was again <10% of that observed in the A_{2A} AR-transfected cell line. However, to ensure unambiguous interpretation of the results from our mutagenesis experiments, all experiments were performed with an untransfected HEK293 cell line in parallel.

Various Binding Site Mutants Are Expressed to Similar Levels in Transiently Transfected HEK293 Cells.

To investigate the mode of binding of LUF5834 compared with CGS21680 a range of A_{2A} AR constructs were generated in which important orthosteric binding site residues were mutated. It was important, therefore, to ensure that such constructs were expressed efficiently in HEK293 cells. Cells were transfected with cDNA of the various mutants. Using an anti-GFP antibody to detect the C-terminal CFP tag, we performed a whole-cell ELISA. We observed that the level of expression of all mutants was comparable with and, in all but one case, greater than that observed for the stably transfected wild-type receptor (Fig. 2A). This indicates that in all cases, the mutant receptors were expressed in this heterologous system. Furthermore, the level of receptor expression for all mutants was similar, between 0.8- and 2 fold-higher compared with the stably expressed wild-type receptor. It should be noted, however, that whereas cells of the stably transfected cell line will all express receptor, the number of cells expressing receptor in the transient transfections is dependent on transfection efficiency. We extended this initial study to look at the functionality of the various mutants compared with the wild-type receptor in terms of their ability

to be activated by a high (100 μ M) concentration of either CGS21680 or LUF5834 (Fig. 2B). With the notable exception of F168^{5.29}D, all mutants showed a higher level of basal and stimulated counts compared with the untransfected cell line underlining that in all cases, the observed signal is derived from the A_{2A} AR variant receptors rather than endogenous A_{2B} ARs. Furthermore, at these high concentrations of ligand, all receptors were activated by one or both of the ligands. This demonstrates that all receptors were expressed and that a significant proportion reached the cell surface.

Residues Interacting with the Heterocyclic Core of ZM241583 or the Adenine Group of Adenosine-Derived Agonists Are Also Important for the Potency of LUF5834.

Several residues such as Asn253^{6.55} and Phe168^{5.29}, which were shown to interact with the heterocyclic core of the antagonist ZM241385 in the A_{2A} AR crystal structure, also play a crucial role in the binding of the agonist 6-(2,2-diphenylethylamino)-9-((2R,3R,4S,5S)-5-(ethylcarbamoyl)-3,4-dihydroxytetrahydrofuran-2-yl)-N-(2-(3-(1-(pyridin-2-yl)piperidin-4-yl)ureido)ethyl)-9H-purine-2-carboxamide (UK432097). However, the role of these residues in the binding and function of nonribose agonists such as LUF5834 has not been determined.

Phe168^{5.29} was shown to be vital for ligand binding contributing a π - π stacking interaction with the heterocyclic core or adenine ring. Mutation of this aromatic residue to the smaller nonaromatic alanine (F168^{5.29}A) caused a >500-fold decrease in potency of CGS21680. A similar decrease in potency was observed for LUF5834 at the F168^{5.29}A variant with a 700-fold decrease in potency indicating that this residue also plays an important role in LUF5834 binding (Table 1; Fig. 3A). Mutation of this residue to an acidic aspartate residue completely abrogated detectable ligand potency. An asparagine residue in helix VI is conserved across all four adenosine receptor subtypes and has been shown to provide a hydrogen bonding interaction with the exocyclic nitrogen of both adenosine-derived agonists and antagonists such as ZM241385. Mutation of this Asn253^{6.55} to alanine caused a

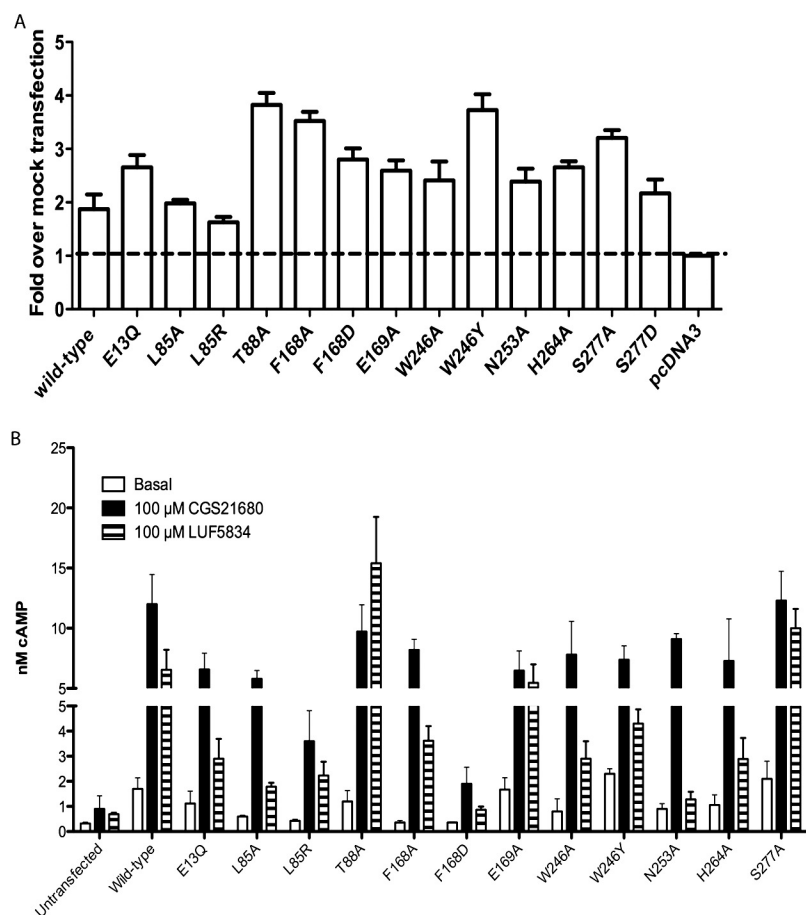


Fig. 2. A, demonstration of total expression levels of the transiently transfected mutant receptors and the stably expressed wild-type receptor in HEK293 cells determined by an ELISA experiment using a monoclonal anti-GFP antibody. B, the ability of 100 μ M CGS21680 (filled columns) or LUF5834 (striped columns) to stimulate cAMP production in HEK293 cells stably transfected with wild-type A_{2A} AR or transiently transfected with mutated A_{2A} AR. Values are expressed as the mean \pm S.E.M. calculated from at least three separate experiments.

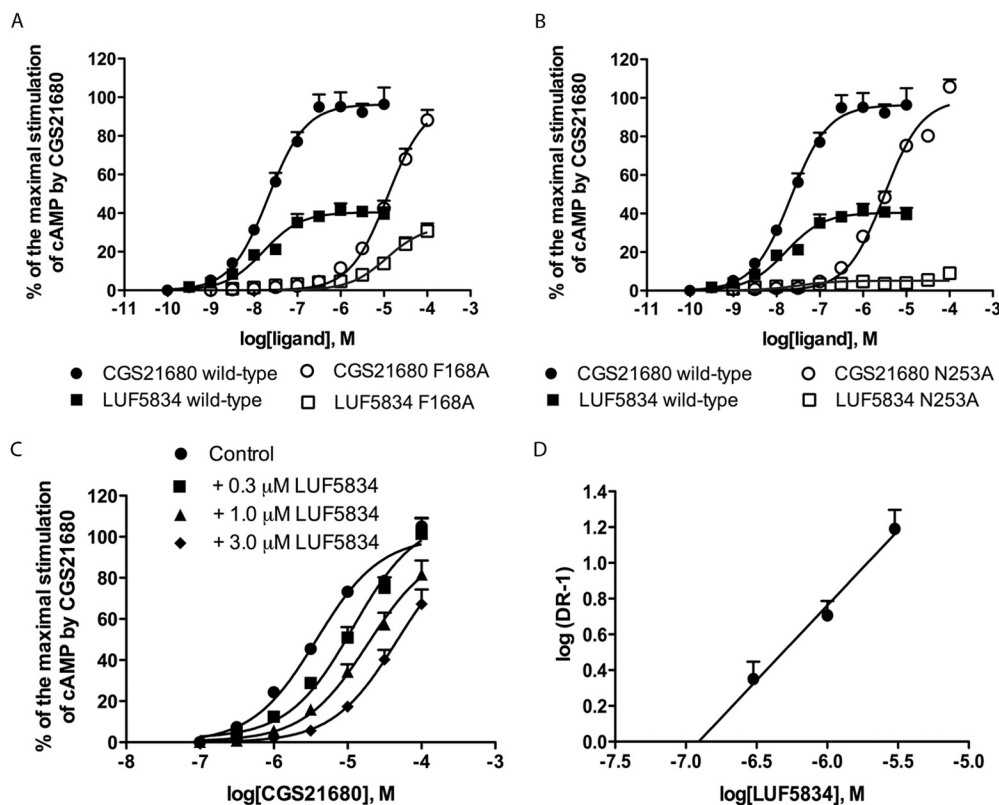


Fig. 3. The ability of increasing concentrations of CGS21680 (circles) or LUF5834 (squares) to stimulate cAMP production in cells stably expressing the wild-type A_{2A} AR (A and B) or the variants F168^{S30}A- A_{2A} AR (A) or N253⁶⁵⁵A- A_{2A} AR (B). The efficacy of LUF5834 is shown as a percentage of that of CGS21680 at the same (wild-type or mutant) receptor. C, the interaction of increasing concentrations of LUF5834 on the dose-response curve of CGS21680 at HEK293 cells expressing the N253⁶⁵⁵A- A_{2A} AR. Data from this experiment was used to construct a Schild plot (D) to enable a determination of the affinity of LUF5834 at this receptor. Values represent mean \pm S.E.M. from at least three separate experiments.

>100-fold decrease in potency for CGS21680 (Table 1; Fig. 3B). It is noteworthy that LUF5834 failed to induce a response at this mutant even at a concentration of 100 μ M. Interaction studies of LUF5834 with CGS21680 were performed to determine whether the mutation of this asparagine residue reduced the affinity or the efficacy of LUF5834. If the latter is correct, then LUF5834 should behave as a classic competitive antagonist with respect to CGS21680. We performed concentration-response curves of CGS21680 in the presence of increasing concentrations of LUF5834 (Fig. 3C). Schild analysis of this experiment revealed LUF5834 does indeed behave like a competitive antagonist as indicated by a Schild-slope of unity (Fig. 3D). Furthermore, the affinity of LUF5834 for the N253^{6,55}A mutant derived from these experiments (pA_2 of 6.9 ± 0.1) was 6-fold lower than the affinity of LUF5834 for the wild-type receptor as determined from the functional data and not significantly different from that observed for the wild-type receptor as determined by displacement of [³H]ZM241385 ($pK_i = 7.1 \pm 0.2$; Table 3). This indicates that the effect of the N253A mutation on the function of LUF5834 is predominantly an effect on ligand efficacy rather than affinity. It should be noted that [³H]ZM241385 binding experiments on the N253^{6,55}A mutation could not be performed because this mutation abrogated detectable [³H]ZM241385 binding.

Mutation of a Glutamate in the Extracellular Loop of the A_{2A} AR Affects Antagonist but Not Agonist Binding. The exocyclic nitrogen of ZM241385 was also shown to form a hydrogen bond with Glu169^{5,30} from ECL2 in the crystal structure. Again, it was of interest to determine whether this residue makes a similar contribution to LUF5834 binding and function. No significant change in potency of either LUF5834 or CGS21680 was observed when Glu169^{5,30} was mutated to alanine (Fig. 4A; Table 1). This

result is incongruous with previous data demonstrating mutation of this residue had a significant effect on both antagonist and agonist binding (Kim et al., 1996). Initial radioligand experiments using membranes expressing the E169A mutation demonstrated that this mutation abrogated [³H]ZM241385 binding when ≤ 20 nM radioligand was used. Consequently, to determine the affinity of ZM241385 for this mutated receptor, we used ligand interaction studies and Schild plot analysis. Concentration response curves of CGS21680 at the E169^{5,30}A mutation were performed in the presence of increasing concentrations of ZM241385 (Fig. 4, B and D). The addition of ZM241385 not only led to rightward shifts of the CGS21680 concentration-response curves, as might be expected for a competitive antagonist, but also caused a significant decrease in basal cAMP production. By performing Schild analysis of the dose-response shifts observed, an estimated value of pK_b of 7.2 ± 0.3 was obtained. This is in agreement with the value of pIC_{50} obtained for the inverse antagonist action of ZM241385 when added alone in increasing concentrations to cells expressing the E169^{5,30}A mutant of the A_{2A} AR (Fig. 4C, $pIC_{50, \text{wild-type}}$, 8.51 ± 0.1 ; $pIC_{50, \text{E169A}}$, 7.04 ± 0.1). Both of these values suggest a 20- to 30-fold loss of affinity of ZM241385 for this mutation in line with previously reported data. His264^{6,66} from ECL3 is near Glu169^{5,30} in the antagonist-bound crystal structure and the agonist-bound structures determined using a thermostabilizing mutagenesis approach (Fig. 5). Mutation of this histidine residue to alanine caused a 4-fold decrease in CGS21680 potency and a 2-fold increase in LUF5834 potency (Table 1).

Agonist Specific Mutations: Mutation of Two "Ribose Interacting" Residues Reduced the Potency of CGS21680 but Not LUF5834. Both Ser277^{7,42} and Thr88^{3,36} were proposed to interact with the ribose group of adenosine-like ligands such as CGS21680 (Kim et al., 2003). This interaction was confirmed by the crystal structures in which adenosine or the adenosine-

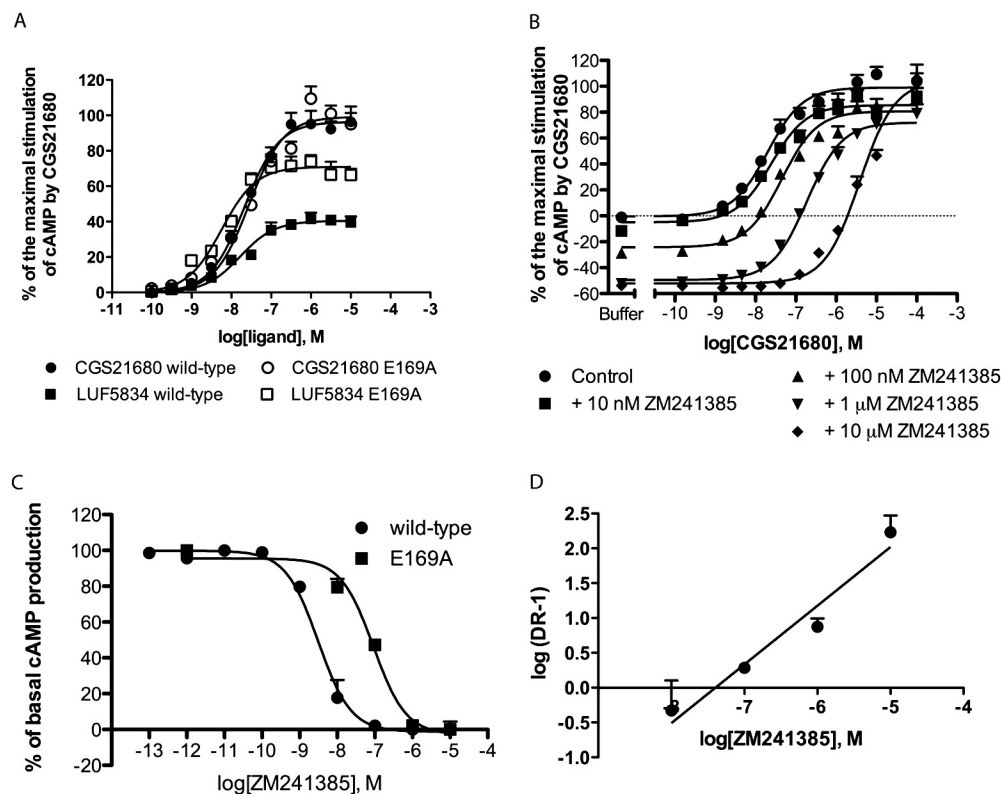


Fig. 4. A, the ability of increasing concentrations of CGS21680 (circles) or LUF5834 (squares) to stimulate cAMP production in cells stably expressing the wild-type A_{2A} AR or the variant E169^{5,30}A-A_{2A} AR. The efficacy of LUF5834 is shown as a percentage of that of CGS21680 at the same (wild-type or mutant) receptor. B, the interaction of increasing concentrations of the antagonist ZM241385 on the dose-response curve of CGS21680 at HEK293 cells expressing the E169^{5,30}A-A_{2A} AR. Data from this experiment was used to construct a Schild plot (D) to enable a determination of the affinity of ZM241385 at this receptor. C, increasing concentrations of ZM241385 were able to reduce the basal cAMP production of HEK293 cells transfected with the E169^{5,30}A-A_{2A} AR mutant. Values represent mean \pm S.E.M. from at least three separate experiments.

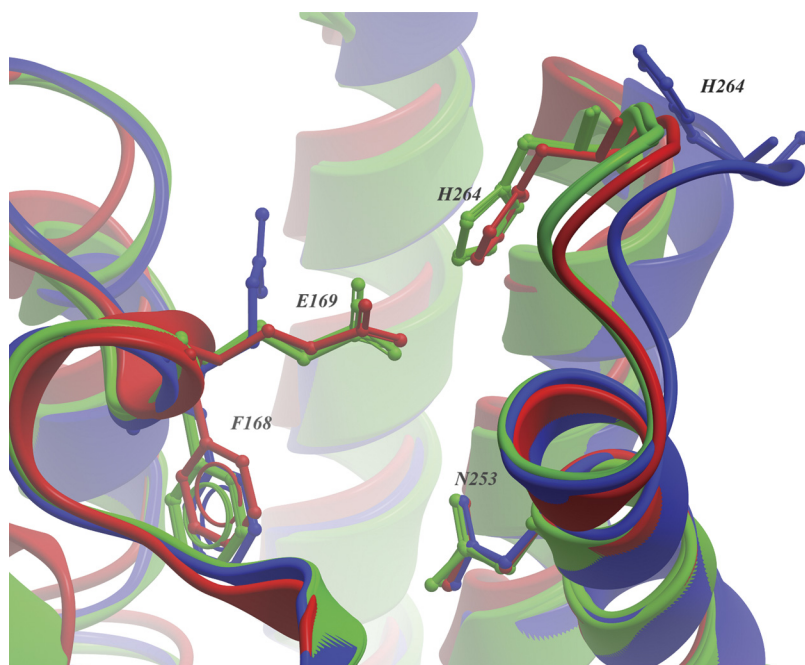


Fig. 5. Crystallographic structure-based molecular models of the human adenosine A_{2A} receptor illustrating the position of Glu169^{5,30}. Four distinct models are shown: 1) a model based on the inactive antagonist bound A_{2A}R-T4L structure (PDB code 3EML) is shown in red; 2 and 3) models based on the thermo-stabilized A_{2A}R active structures bound to adenosine or NECA (PDB codes 2YDO and 2YDV, respectively) shown in green with Glu169 and His264 in close proximity; and 4) a model based on the A_{2A}R-T4L cocrystallized with the agonist UK432097 (PDB code 3QAK) showing a reorientation of Glu169 away from His264, displayed in blue.

derived agonists UK432097 and NECA was cocrystallized (Lebon et al., 2011; Xu et al., 2011). Although LUF5834 has no ribose group, it does contain several exocyclic amine and nitrile groups next to a hydroxyl group, all capable of making hydrogen-bonding interactions. Mutation of Thr88^{3,36} and Ser277^{7,42} to alanine caused a 1700- and 110-fold decrease in CGS21680 potency (Table 1; Fig. 6A). Conversely, LUF5834 potency was not reduced by either mutation, and rather a slight increase in potency was observed at the S277^{7,42}A mutation. Furthermore, an increase in efficacy of LUF5834 compared with CGS21680 was seen for this mutation (LUF5834 $E_{\max, \text{wild-type}} = 41\%$ of

CGS21680; LUF5834 $E_{\max, \text{S277A}} = 94\%$). Potency of a ligand is derived from both affinity and efficacy. Therefore, we wanted to ascertain whether the effects of the above mutations upon CGS21680 potency were driven by a loss of affinity. To achieve this, we first determined the affinity of [³H]ZM241385 for the two mutant receptors using a homologous competition binding assay and membranes of HEK293 cells expressing either T88^{3,36}A-A_{2A} AR or S277^{7,42}A-A_{2A} AR (Table 2). Compared with the wild-type receptor, neither mutation caused any decrease in [³H]ZM241385 affinity. In line with the ELISA data, the level of expression of the T88^{3,36}A and S277^{7,42}A mutations

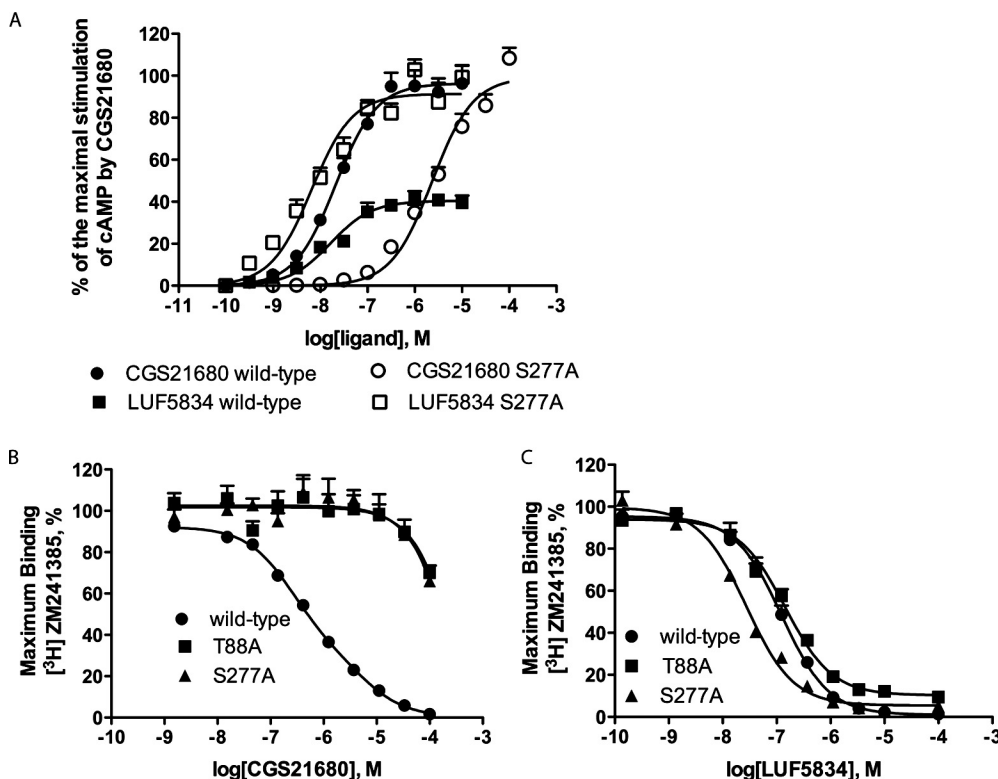


Fig. 6. A, the ability of increasing concentrations of CGS21680 (circles) or LUF5834 (squares) to stimulate cAMP production in cells stably expressing the wild-type A_{2A} AR or the variant S277^{7,42}A-A_{2A} AR. The efficacy of LUF5834 is shown as a percentage of that of CGS21680 at the same (wild-type or mutant) receptor. The affinity of [³H]ZM241385 was unchanged at the S277^{7,42}A-A_{2A} AR or T88^{3,36}A-A_{2A} AR (Table 2). Using competition binding of [³H]ZM241384 versus CGS21680 (B) or LUF5834 (C), values of affinity for these ligands at the wild-type (circles), T88^{3,36}A (squares), or S277^{7,42}A (triangles) A_{2A} AR. Values represent mean \pm S.E.M. from at least three separate experiments.

TABLE 2

The affinities of [³H]ZM241385 and the B_{\max} values of wild-type, T88^{3.36}A mutant, and S277^{7.42}A mutant adenosine A_{2A} receptors determined with a homologous competition binding assay

The table shows the mean \pm S.E.M. calculated from three independent experiments, each performed in duplicate. No significant differences were observed between the K_D values of the different constructs according to an unpaired t test. Change is expressed as the fold increase in the K_D value for the mutant over that for WT.

Construct	pK_D (K_D)	Change	B_{\max}
	<i>nM</i>	<i>fold</i>	<i>fmol/mg protein</i>
Wild-type	8.5 \pm 0.1 (3.4)	1.0	4840 \pm 556
T88 ^{3.36} A	8.5 \pm 0.0 (3.1)	0.9	11,400 \pm 1470
S277 ^{7.42} A	8.5 \pm 0.0 (2.9)	0.9	15,500 \pm 1760

was 2- to 3-fold that of the wild-type receptor. Using these affinity values for ZM241385, we were then able to use competition assays of [³H]ZM241385 versus CGS21680 or LUF5834 to derive values of K_i for these ligands at both the wild-type and mutant receptors (Fig. 6, B and C; Table 3). These experiments revealed that the displacement of [³H]ZM241385 by LUF5834 was best fit by a single site and that the affinity was unaffected by the mutation of T88^{3.36}A and enhanced >4-fold by the mutation of S277^{7.42}A in line with our functional data. CGS21680 displaced [³H]ZM241385 at the wild-type A_{2A} AR, and this displacement revealed distinct high- and low-affinity sites. However, upon mutation of either Thr88^{3.36} or Ser277^{7.42} to alanine, CGS21680 was unable to displace [³H]ZM241385, indicating a >1000-fold loss of affinity in line with our functional data. Mutation of Glu13^{1.39} in TM1 has been shown to have an effect on agonist but not antagonist binding at the A_{2A} AR. Mutation of this residue to Gln caused a significant decrease in the potency of CGS21680 but caused a slight increase in LUF5834 potency (Table 1).

The Lower Binding Pocket: Mutation of a Hydrophobic Leucine or the Conserved “Toggle Switch” Tryptophan Has Distinct Effects on the Potency of CGS21680 Compared with LUF5834. In the antagonist-bound crystal structure, Leu85 makes a hydrophobic interaction with the furan ring of ZM241385. Likewise, the recent agonist-bound structure by Xu et al. (2011) revealed that Leu85^{3.33} makes a hydrophobic interaction with the ribose part of UK432097. Mutation of this residue to the smaller alanine caused an 80-fold reduction of potency for CGS21680, whereas no detectable signal could be observed for LUF5834 (Table 1). Likewise, mutation of this Leu to an Arg, thus introducing a charge but somewhat increasing the size of the residue caused a >600-fold reduction in CGS21680 potency, whereas LUF5834 potency was reduced by 26-fold (Table 1). The highly conserved tryptophan (Trp246^{6.48}) has been implicated as a key player in class A GPCR activation acting as a toggle switch. Consequently, it was of interest to monitor the

influence of this residue upon CGS21680 and LUF5834 potency. Mutation of this large aromatic residue to the smaller nonaromatic alanine caused a decrease in CGS21680 potency but a modest 3-fold increase in LUF5834 potency, whereas the efficacy of LUF5834 compared with CGS21680 remained unchanged (Table 1). Mutation of this tryptophan to tyrosine, thus maintaining the aromatic nature of the residue, did not change the potency of CGS21680 compared with the wild type. We were surprised, however, that this mutation caused an increase of >10-fold in the potency of LUF5834 while maintaining its relative efficacy compared with CGS21680 (Table 1).

Molecular Modeling. The mutagenesis experiments reveal that although LUF5834 and CGS21680 may occupy a similar and overlapping binding pocket, the residues that they interact with to exert their agonistic effect are most likely distinct. This was further investigated using molecular docking studies using both the antagonist- and agonist-bound crystal structures as templates. In docking studies using the UK432097-bound structure as a template residues within a 7.5-Å sphere around the ligand were selected as binding pocket. The docking results gave a single plausible binding pose for both CGS21680 and LUF5834 (Fig. 7).

The pose found for CGS21680 was very similar to the cocrystallized ligand as would be expected based on their high chemical similarity (Fig. 7, A and C). CGS21680 had π - π stacking interaction between the adenine core and Phe168 and a cation- π interaction to Leu249^{6.51}. The bicyclic core also forms two hydrogen bonds to Asn253^{6.55}. Furthermore, its ribose group formed hydrogen bonds to residues Thr88^{3.36}, His250^{6.52}, Ser277^{7.42}, and His278^{7.43} in the lower binding pocket, comparable with the cocrystallized ligand UK432097 (Xu et al., 2011). Finally, a hydrogen bond is formed between the terminal carboxyl group and Tyr 271^{7.36}.

The LUF5834 binding pose shows the hydroxyphenyl group directed into the binding pocket (Fig. 7, B and D). LUF5834 forms a cation- π interaction between the pyridine core of LUF5834 and Phe168^{5.30}, which is much smaller than the π - π stacking between CGS21680 and Phe168^{5.30} because of the smaller pyridine core. However, Phe168^{5.30}, along with Leu249^{6.51}, plays a key part in aligning the core of the molecule to enable the formation of hydrogen bonds to Asn253^{6.55} and a water-mediated hydrogen bond to Ala63^{2.61} and Tyr9^{1.35} (Fig. 7D) via a water molecule. These hydrogen bonds, including the water-mediated bond to the amide carbonyl of Ala63^{2.61} (Fig. 7C), are also formed by the cocrystallized agonist. In the agonist-bound structure, if this bond is not present, Tyr9^{1.35} forms a hydrogen bond to Glu13^{1.39}. Because of the key role Phe168^{5.30} plays, this pose is in line

TABLE 3

Ligand binding properties of wild-type, T88^{3.36}A mutant, and S277^{7.42}A mutant adenosine A_{2A} receptors characterized in [³H]ZM241385 binding assays in competition with CGS21680 and LUF5834

The table shows the mean \pm S.E.M. calculated from three independent experiments, each performed in duplicate. No significant differences were observed between the pK_i values of LUF5834 on the different constructs according to an unpaired t test. Change is expressed as the fold increase in the K_i value for the mutant over that for WT.

Construct	CGS21680			LUF5834	
	pK_i High (K_i High)	pK_i Low (K_i Low)	Change	pK_i (K_i)	Change
	<i>nM</i>		<i>fold</i>	<i>nM</i>	<i>fold</i>
Wild-type	6.8 \pm 0.1 (159)	5.4 \pm 0.1 (3680)	1.0	7.1 \pm 0.2 (79.6)	1.0
T88 ^{3.36} A	N.D.	N.D.	>1000	6.9 \pm 0.1 (127)	1.6
S277 ^{7.42} A	N.D.	N.D.	>1000	7.8 \pm 0.0 (17.7)	0.2

N.D., not determined; the potency was too low to determine an accurate EC₅₀ value.

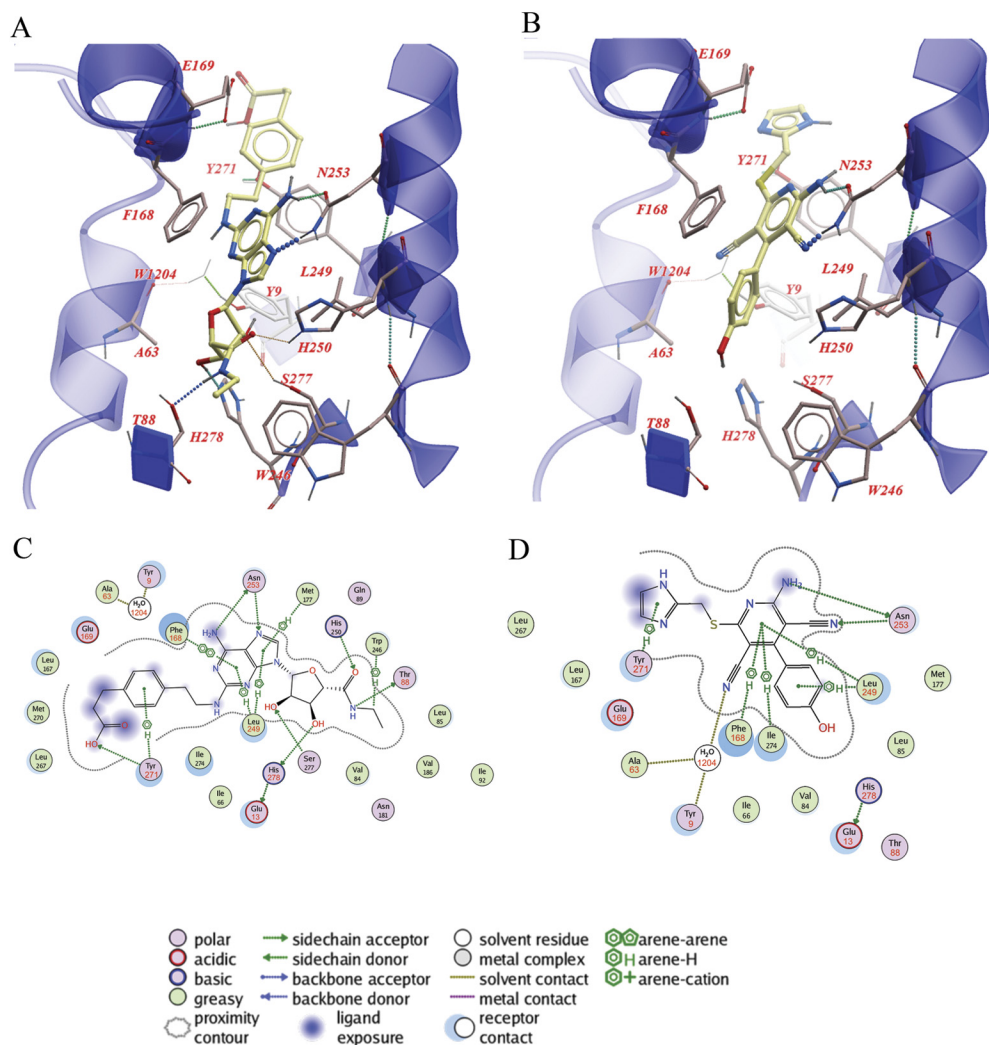


Fig. 7. Crystallographic structure-based molecular models of the human adenosine A_{2A} receptor containing CGS21680 (A) and LUF5834 (B). Results of the docking study of LUF5834 using a model based on the agonist bound A_{2A} AR structure (PDB code 3QAK). The models represent the most feasible pose for both CG21680 and LUF5834. On the left, the docking pose of CGS21680 is shown in three (A) and two (C) dimensions, whereas on the right, the docking pose of LUF5834 is shown where the hydroxyl phenyl group is directed into the binding pocket in three (B) and two (D) dimensions. Residues described in the main text are shown in red.

with the large effect observed upon mutation of Phe168^{5,30} to alanine. Ser277^{7,42} and Thr88^{3,36} make no direct contact with the ligand, in agreement with the functional data from the mutagenesis studies. More importantly, the hydroxyphenyl group is located very near to Trp246^{6,48}. In the wild-type receptor, this hydroxyphenyl group is involved only in a cation- π interaction to Leu246^{6,51}. However, it can be speculated that the mutation of Trp246 to a tyrosine enables the formation of a hydrogen bond between Tyr246^{6,48} and the hydroxyphenyl group. This would increase the binding affinity of LUF5834, which is in line with the experimental results. In addition, this pose shows no direct interaction with Glu169^{5,30}, indicating that mutation of this residue would have little effect on the binding of LUF5834 to the receptor, as was observed in this study. In addition, a low-energy cation- π interaction is formed between the imidazole group and the hydrogen of the hydroxyl group on Tyr 271^{7,36}.

Mutation of Glu13^{1,39} in TM1 has been shown to have an effect on agonist but not antagonist binding at the A_{2A} AR (IJzerman et al., 1996; Gao et al., 2000). Our modeling studies highlight a role for this residue in agonist binding (Fig. 8). In both the CGS21680- and LUF5834-bound models, this residue is shown to stabilize His278^{7,43} via a hydrogen bond. It is noteworthy that this interaction is present in all crystal structures of agonist bound A_{2A} ARs to date (PDB numbers

3QAK, 2YDV, and 2YDO) but not in antagonist bound structures (PDB numbers 3EML, 3RFM, 3REY, 3PWH; data not shown). Given the importance of His278^{7,43} in providing a hydrogen-bond interaction with the ribose group of adenosine-derived agonists, the decrease in CGS21680 potency observed upon mutation of Glu13^{1,39} would be expected (Fig. 8A). Conversely, LUF5834, which lacks a ribose group, makes no such interaction with His278^{7,43} and is therefore unaffected by the E13^{1,39}A mutation (Fig. 8B). This lack of interaction is due mainly to the positioning of the hydroxyl group on the aromatic group of LUF5834, preventing a productive hydrogen bond from being formed with the fixed residue His278^{7,43}. However, it could be speculated that this interaction is possible when residue His278^{7,43} can move more freely, as would be the case in the E13^{1,39}A mutation. However, LUF5834 does form a hydrogen bond via a water molecule to Tyr9^{1,35} located next to Glu13^{1,39}.

Discussion

In the past, synthetic agonists of the adenosine receptors have all been derivatives of the endogenous ligand adenosine, and the ribose moiety conserved in all these ligands was thought to be essential for agonist efficacy (Soudijn et al., 2003). In this study, we have used one such ligand,

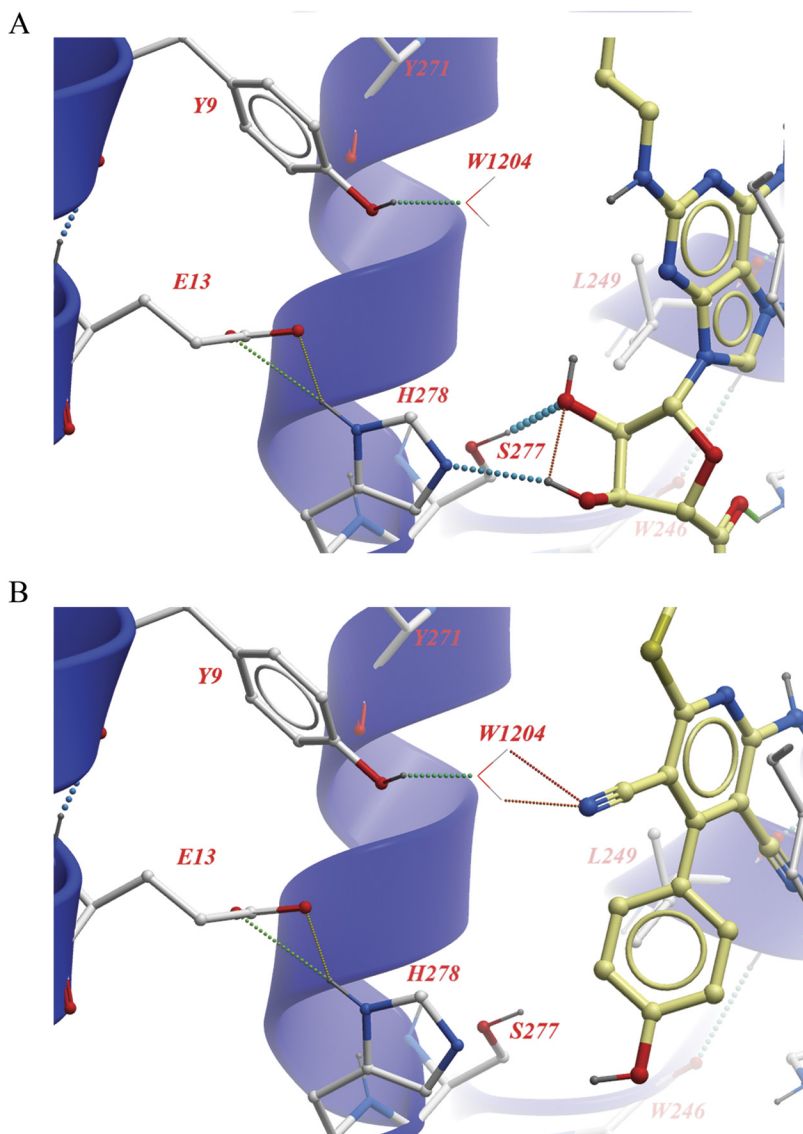


Fig. 8. Crystallographic structure-based molecular models of the human adenosine A_{2A} receptor containing CGS21680 (A) and LUF5834 (B). Results of the docking study of LUF5834 using a model based on the agonist bound A_{2A} AR structure (PDB code 3QAK). The models represent the most feasible pose for both CGS21680 and LUF5834 and highlights the role of Glu13^{1,39} in coordinating His278^{7,43} with a hydrogen bond. Furthermore, the ribose group of CGS21680 makes a hydrogen bond interaction with the ribose group of CGS21680 (A), whereas no such interaction is observed for LUF5834 (B).

CGS21680, a high-affinity selective agonist for the A_{2A} AR with a (2-carboxyethyl)phenylethylamino group at the C2 position and an *N*-ethylcarboxamido group at the C5' (Fig. 1). However, a number of Bayer patents, such as those by Rosenreter et al. (2001, 2003), reveal a novel class of adenosine receptor ligands with significant affinity and efficacy but lacking a ribose group, namely a series of 2-amino-4,6-disubstituted pyridine-3,5-dicarbonitriles. In the present study, we first confirmed that one such compound, LUF5834, is a potent partial agonist at the A_{2A} AR.

The recently published structure of the A_{2A} AR cocrystallized with the agonist UK432097, an analog of CGS21680, confirms the importance of the ribose group for agonist function (Xu et al., 2011). Two residues in helix VII, Ser277^{7,42} and His278^{7,43}, together with the side chain of Thr88^{3,36}, form a hydrogen-bonding network coordinating the ribose moiety. This relatively subtle interaction resulted in a seesaw-like movement of helix VII around the ribose ring, shifting the intracellular part of helix VII 4 or 5 Å inward. In helix III, coordination of the ribose moiety in UK432097 through a hydrogen bonding interaction between the 5'-*N*-ethyluro- namide substitution and Thr88^{3,36} as well as nonpolar con-

tacts with Leu85^{3,33} caused an upward shift of the entire helix III along its axis (Xu et al., 2011). Mutation of Ser277^{7,42}, Thr88^{3,36}, and Leu85^{3,33} to alanine abrogated this agonist interaction and reduced the potency and affinity of CGS21680 by at least 100-fold in agreement with previous studies (Kim et al., 1995; Gao et al., 2000; Ivanov et al., 2009). In contrast, the potency and affinity of LUF5834 were unaffected by the mutation of either Ser277^{7,42} or Thr88^{3,36} to alanine. We extended this study to other residues known to be critical for adenosine-like agonist binding and function. Similar to CGS21680, LUF5834 showed a decreased potency when Leu85^{3,33} was mutated to arginine, and mutation of this residue to alanine completely abrogated LUF5834 function at the A_{2A} AR. This suggests that although LUF5834 does not interact with Thr88, a nonpolar interaction with TM3 residues is still crucial for its agonistic function. The mutation E13^{1,39}A has previously been shown to decrease agonist but not antagonist binding affinity (Ijzerman et al., 1996; Gao et al., 2000). In the present study, a 6-fold decrease in CGS21680 potency was observed, whereas LUF5834 displayed a 3-fold increase in potency. Our molecular modeling studies highlight a role for this residue in agonist binding,

whereby Glu13^{1.39}, rather than interacting directly with the ligand, coordinates His278^{7.43} with a hydrogen bond as suggested in a previous mutagenesis and modeling study (Jozerman et al., 1996). LUF5834 makes no interaction with His278^{7.43} and is accordingly unaffected by the mutation of Glu13^{1.39} to alanine.

Previous pharmacological characterization of [³H]LUF5834 at the A₁ AR suggested that this ligand has an overlapping orthosteric binding mode with respect to both the xanthine-derived antagonist 8-cyclopentyl-1,3-dipropylxanthine and the adenosine-derived agonist 2-chloro-*N*⁶-cyclopentyladenosine (Lane et al., 2010). Mutation of the highly conserved Phe168^{5.30} in ECL2 reduced the potency of both CGS21680 and LUF5834. This suggests that both the adenine core of CGS21680 and the pyridine core of LUF5834 make direct interactions with Phe168^{5.30} consistent with our docking studies. Asn253^{6.55} makes an important interaction with the exocyclic nitrogen that extends from the heterocyclic core of ZM241385 and the adenine ring of UK432097 (Kim et al., 1995; Jaakola et al., 2008; Xu et al., 2011). Mutation of this residue greatly decreased potency of CGS21680, whereas LUF5834 showed a moderate loss of affinity and a complete loss of agonist efficacy. It is important to note that LUF5834 is a partial agonist compared with CGS21680. An early study on the β_2 adrenergic receptor demonstrated that mutation of N293^{6.55}L in the receptor caused a loss of affinity for a range of agonists that was strongly correlated with the intrinsic activity of the ligand; full agonists showed a >10-fold loss of affinity, whereas partial agonists had almost the same affinity for this mutant receptor (Wieland et al., 1996). More recently, both NMR spectroscopy studies and the agonist-bound crystal structures of the β_2 adrenergic receptor have revealed that an inward movement of TM6 permits the interaction of Asn293^{6.55} with agonists changing the receptor to an active conformation (Bokoch et al., 2010; Rasmussen et al., 2011; Rosenbaum et al., 2011; Warne et al., 2011). Finally, His393^{6.55} has been shown to be a determinant of stimulus bias at the dopamine D₂ receptor (Tschammer et al., 2011). Therefore, this residue is a key determinant of ligand efficacy at these receptors. It can be speculated that the findings in this study can be related to a simple model of receptor activation with an inactive and an active state of the receptor, whereby the mutation of N253A^{6.55} stabilizes an inactive conformation of the receptor. As a partial agonist, LUF5834 will bind with a similar affinity to this mutated receptor, although a loss of efficacy will be observed (Christopoulos and Kenakin, 2002).

Glu169^{5.30} in ECL2 was highlighted as having a key role in ligand binding by ligand docking, mutagenesis studies, and finally the antagonist-bound crystal structure (Kim et al., 1996; Jaakola et al., 2008; Ivanov et al., 2009). Consistent with these observations, we observed a >20-fold reduction in the affinity of [³H]ZM241385. However, in functional assays, the potency of CGS21680 was unchanged compared with the wild type, and the potency of LUF5834 was slightly (2-fold) enhanced. This is particularly surprising for CGS21680, in which the exocyclic nitrogen of the adenine core would be expected to play a role similar to that of the exocyclic nitrogen in ZM241385 and interact with this residue via a hydrogen bond. However, in the structure of the A_{2A} AR cocrystallized with UK432097, this glutamate residue does not make a hydrogen-bonding interaction with the exocyclic nitrogen from the adenine core of this agonist because of a bulky substitution at this area (Xu et al.,

2011). Rather, Glu169^{5.30} interacts with the urea group of the 2-(3-(1-(pyridin-2-yl)piperidin-4-yl)ureido)ethylcarboxamido substitution. This suggests that an interaction between Glu169 and the exocyclic nitrogen of an adenosine-like agonist is not essential for agonist function. Molecular modeling suggests that Glu169^{5.30} forms a hydrogen-bonding interaction with His264^{6.66} from ECL3 in the antagonist-bound inactive structure, which is completely absent in the UK432097 cocrystallized active structure. However, Lebon et al. (2011) have cocrystallized the two agonists NECA and adenosine with the A_{2A} AR, showing that both these agonists interact significantly with Glu169^{5.30}. However, the authors suggest that these structures represent partially activated receptor structures, observing that the structural changes occurring at the cytoplasmic side of the receptor are too small to allow interaction with a G protein. The important role of the extracellular loops in the activation of GPCRs has been illustrated by mutagenesis and NMR studies (Bokoch et al., 2010; Peeters et al., 2011). It is tempting to speculate that the breaking of the interaction between Glu169^{5.30} and His264^{6.66} and the movement of Glu169^{5.30} away from the ligand binding site also represent a key step in receptor activation that is not observed in these partially active agonist-bound structures.

A predominant feature common among opsin, the β_2 adrenergic receptor, and the agonist bound A_{2A} AR, compared with their “inactive” counterparts, is the overall movement of helices V and VI (Scheerer et al., 2008; Rasmussen et al., 2011; Xu et al., 2011). However, contrary to the previously proposed toggle-switch mechanism (Shi et al., 2002), these studies revealed that the conserved Trp^{6.48} does not undergo a rotamer transition; rather, it moves along with the backbone of helix VI. In the present study, mutation of this residue to an alanine greatly reduced CGS21680 potency but actually increased LUF5834 potency. Mutation of this tryptophan to an aromatic tyrosine residue preserved the potency of CGS21680 and caused a remarkable >10-fold increase in LUF5834 potency. A recent mutagenesis study of the serotonin 5HT₄ receptor demonstrate that Trp^{6.48} is not required for activation of this receptor by serotonin (Pellissier et al., 2009). Studies on the β_2 adrenergic receptor have proposed that full but not partial agonists require this residue for their action (Swaminath et al., 2005).

In conclusion, there have been differential, even opposite, effects of various mutants throughout this study on these two structurally distinct agonists. Schwartz and coworkers have introduced the concept of distinct microswitches forming an extended allosteric interface between the transmembrane helices performing the global toggle switch movements that mediate transduction of a signal across the receptor (Holst et al., 2010). Thus agonist ligands binding at the same receptor and even occupying an overlapping binding site may stabilize distinct conformations of the receptor and activate the receptor by distinct mechanisms, engaging distinct “switches.” Agonist-specific conformations of receptors have been associated with the paradigm of stimulus-bias (Kenakin and Miller, 2010). Crystallographic studies using a single receptor with a range of structurally distinct or stimulus-biased agonists will provide important information toward the heterogeneity of such activation mechanisms. In that light, our study may serve as a prelude to such efforts.

Acknowledgments

We thank Thea Mulder-Krieger for technical assistance and Alwin Hendriks for preliminary molecular modeling studies.

Authorship Contributions

Participated in research design: Lane, van Westen, Hoffmann, and IJzerman.

Conducted experiments: Lane, Klein Herenbrink, van Westen, and Spoorendronk.

Contributed new reagents or analytic tools: Hoffmann.

Performed data analysis: Lane, Klein Herenbrink, and van Westen.

Wrote or contributed to the writing of the manuscript: Lane, Klein Herenbrink, van Westen, Hoffmann, and IJzerman.

References

- Beukers MW, Chang LC, van Frijtag Drabbe Künzel JK, Mulder-Krieger T, Spanjersberg RF, Brussee J, and IJzerman AP (2004) New, non-adenosine, high-potency agonists for the human adenosine A2B receptor with an improved selectivity profile compared to the reference agonist N-ethylcarboxamidoadenosine. *J Med Chem* **47**:3707–3709.
- Black JW and Leff P (1983) Operational models of pharmacological agonism. *Proc R Soc Lond B Biol Sci* **220**:141–162.
- Bokoch MP, Zou Y, Rasmussen SG, Liu CW, Nygaard R, Rosenbaum DM, Fung JJ, Choi HJ, Thian FS, Kobilka TS, et al. (2010) Ligand-specific regulation of the extracellular surface of a G-protein-coupled receptor. *Nature* **463**:108–112.
- Chang LC, van Frijtag Drabbe Künzel JK, Mulder-Krieger T, Spanjersberg RF, Roerink SF, van den Hout G, Beukers MW, Brussee J, and IJzerman AP (2005) A series of ligands displaying a remarkable agonistic-antagonistic profile at the adenosine A1 receptor. *J Med Chem* **48**:2045–2053.
- Cheng Y and Prusoff WH (1973) Relationship between the inhibition constant (K_i) and the concentration of inhibitor which causes 50 per cent inhibition (I₅₀) of an enzymatic reaction. *Biochem Pharmacol* **22**:3099–3108.
- Christopoulos A and Kenakin T (2002) G protein-coupled receptor allostery and complexing. *Pharmacol Rev* **54**:323–374.
- Cooper J, Hill SJ, and Alexander SP (1997) An endogenous A2B adenosine receptor coupled to cyclic AMP generation in human embryonic kidney (HEK 293) cells. *Br J Pharmacol* **122**:546–550.
- Fredholm BB, IJzerman AP, Jacobson KA, Linden J, and Müller CE (2011) International Union of Basic and Clinical Pharmacology. LXXXI. Nomenclature and classification of adenosine receptors—an update. *Pharmacol Rev* **63**:1–34.
- Gao ZG, Jiang Q, Jacobson KA, and IJzerman AP (2000) Site-directed mutagenesis studies of human A(2A) adenosine receptors: involvement of glu(13) and his(278) in ligand binding and sodium modulation. *Biochem Pharmacol* **60**:661–668.
- Giles H, Lansdell SJ, Bollo ML, Wilson HL, and Martin GR (1996) Characterization of a 5-HT_{1B} receptor on CHO cells: functional responses in the absence of radioligand binding. *Br J Pharmacol* **117**:1119–1126.
- Heitman LH, Mulder-Krieger T, Spanjersberg RF, van Frijtag Drabbe Künzel JK, Dalpiaz A, and IJzerman AP (2006) Allosteric modulation, thermodynamics and binding to wild-type and mutant (T277A) adenosine A1 receptors of LUF5831, a novel nonadenosine-like agonist. *Br J Pharmacol* **147**:533–541.
- Hoffmann C, Gaietta G, Bünnemann M, Adams SR, Oberdorff-Maass S, Behr B, Vilardaga JP, Tsien RY, Ellisman MH, and Lohse MJ (2005) A FRET-based FRET approach to determine G protein-coupled receptor activation in living cells. *Nat Methods* **2**:171–176.
- Holst B, Nygaard R, Valentin-Hansen L, Bach A, Engelstoft MS, Petersen PS, Frimurer TM, and Schwartz TW (2010) A conserved aromatic lock for the tryptophan rotameric switch in TM-VI of seven-transmembrane receptors. *J Biol Chem* **285**:3973–3985.
- IJzerman AP, Von Frijtag Drabbe Künzel JK, Kim J, Jiang Q, and Jacobson KA (1996) Site-directed mutagenesis of the human adenosine A2A receptor. Critical involvement of Glu13 in agonist recognition. *Eur J Pharmacol* **310**:269–272.
- Ivanov AA, Barak D, and Jacobson KA (2009) Evaluation of homology modeling of G-protein-coupled receptors in light of the A(2A) adenosine receptor crystallographic structure. *J Med Chem* **52**:3284–3292.
- Jaakola VP, Griffith MT, Hanson MA, Cherezov V, Chien EY, Lane JR, IJzerman AP, and Stevens RC (2008) The 2.6 angstrom crystal structure of a human A2A adenosine receptor bound to an antagonist. *Science* **322**:1211–1217.
- Jaakola VP, Lane JR, Lin JY, Katritch V, IJzerman AP, and Stevens RC (2010) Ligand binding and subtype selectivity of the human A(2A) adenosine receptor: identification and characterization of essential amino acid residues. *J Biol Chem* **285**:13032–13044.
- Jacobson KA and Gao ZG (2006) Adenosine receptors as therapeutic targets. *Nat Rev Drug Discov* **5**:247–264.
- Jacobson KA, Ohno M, Duong HT, Kim SK, Tchilibon S, Cesnek M, Holý A, and Gao ZG (2005) A neoreceptor approach to unraveling microscopic interactions between the human A2A adenosine receptor and its agonists. *Chem Biol* **12**:237–247.
- Jiang Q, Van Rhee AM, Kim J, Yehle S, Wess J, and Jacobson KA (1996) Hydrophilic side chains in the third and seventh transmembrane helical domains of human A2A adenosine receptors are required for ligand recognition. *Mol Pharmacol* **50**:512–521.
- Kenakin T and Miller LJ (2010) Seven transmembrane receptors as shapeshifting proteins: the impact of allosteric modulation and functional selectivity on new drug discovery. *Pharmacol Rev* **62**:265–304.
- Kim J, Jiang Q, Glashofer M, Yehle S, Wess J, and Jacobson KA (1996) Glutamate residues in the second extracellular loop of the human A2a adenosine receptor are required for ligand recognition. *Mol Pharmacol* **49**:683–691.
- Kim J, Wess J, van Rhee AM, Schöneberg T, and Jacobson KA (1995) Site-directed mutagenesis identifies residues involved in ligand recognition in the human A_{2A} adenosine receptor. *J Biol Chem* **270**:13987–13997.
- Kim SK, Gao ZG, Van Rompaey P, Gross AS, Chen A, Van Calenbergh S, and Jacobson KA (2003) Modeling the adenosine receptors: comparison of the binding domains of A2A agonists and antagonists. *J Med Chem* **46**:4847–4859.
- Kobilka BK (2011) Structural insights into adrenergic receptor function and pharmacology. *Trends Pharmacol Sci* **32**:213–218.
- Lane JR, Klaasse E, Lin J, van Bruchem J, Beukers MW, and IJzerman AP (2010) Characterization of [³H]LUF5834: a novel non-ribose high-affinity agonist radioligand for the adenosine A1 receptor. *Biochem Pharmacol* **80**:1180–1189.
- Lebon G, Warne T, Edwards PC, Bennett K, Langmead CJ, Leslie AG, and Tate CG (2011) Agonist-bound adenosine A2A receptor structures reveal common features of GPCR activation. *Nature* **474**:521–525.
- Miyamoto MI, Clarke KA, Thomas GS, and Belardinelli L (2009) An example of the clinical selectivity of regadenoson for the A2a adenosine receptor. *Am Heart Hosp J* **7**:E118–E121.
- Peeters MC, van Westen GJ, Guo D, Wisse LE, Müller CE, Beukers MW, and IJzerman AP (2011) GPCR structure and activation: an essential role for the first extracellular loop in activating the adenosine A2B receptor. *FASEB J* **25**:632–643.
- Pellissier LP, Sallander J, Campillo M, Gaven F, Queffelecoul E, Pillot M, Dumuis A, Claeysen S, Bockaert J, and Pardo L (2009) Conformational toggle switches implicated in basal constitutive and agonist-induced activated states of 5-hydroxytryptamine-4 receptors. *Mol Pharmacol* **75**:982–990.
- Rasmussen SG, Choi HJ, Fung JJ, Pardon E, Casarosa P, Chae PS, Devree BT, Rosenbaum DM, Thian FS, Kobilka TS, et al. (2011) Structure of a nanobody-stabilized active state of the β (2) adrenoceptor. *Nature* **469**:175–180.
- Rosenbaum DM, Zhang C, Lyons JA, Holl R, Aragao D, Arlow DH, Rasmussen SG, Choi HJ, Devree BT, Sunahara RK, et al. (2011) Structure and function of an irreversible agonist- β (2) adrenoceptor complex. *Nature* **469**:236–240.
- Rosentreter U, Henning R, Bauser M, Kraemer T, Vaupel A, Huebsch W, Dembowski K, Salcher-Schraufstaetter O, Stasch J, Krahn T, et al. (2001), inventors; Bayer Aktiengesellschaft, Rosentreter U, Henning R, Bauser M, Kraemer T, Vaupel A, Huebsch W, Dembowski K, Salcher-Schraufstaetter O, Stasch J, Krahn T, et al., assignees. Substituted 2-thio-3,5-dicyano-4-aryl-6-aminopyridines and the use thereof as adenosine receptor ligands. World patent WO01025210. 2001 Apr 12.
- Rosentreter U, Kraemer T, Shimada M, Huebsch W, Diedrichs N, Krahn T, Henninger K, and Stasch J (2003), inventors; Bayer Aktiengesellschaft, Rosentreter U, Kraemer T, Shimada M, Huebsch W, Diedrichs N, Krahn T, Henninger K, and Stasch J, assignees. Preparation of 2-heteroaryl-methylthio-3,5-dicyano-4-phenyl-6-aminopyridines as adenosine receptor selective ligands. World patent WO03008384. 2003 Jan 30.
- Scheerer P, Park JH, Hildebrand PW, Kim YJ, Krauss N, Choe HW, Hofmann KP, and Ernst OP (2008) Crystal structure of opsin in its G-protein-interacting conformation. *Nature* **455**:497–502.
- Shi L, Liapakis G, Xu R, Guarnieri F, Ballesteros JA, and Javitch JA (2002) Beta2 adrenergic receptor activation. Modulation of the proline kink in transmembrane 6 by a rotamer toggle switch. *J Biol Chem* **277**:40989–40996.
- Soudijn W, van Wijngaarden I, and IJzerman AP (2003) Medicinal chemistry of adenosine A1 receptor ligands. *Curr Top Med Chem* **3**:355–367.
- Swaminath G, Deupi X, Lee TW, Zhu W, Thian FS, Kobilka TS, and Kobilka B (2005) Probing the β 2 adrenoceptor binding site with catechol reveals differences in binding and activation by agonists and partial agonists. *J Biol Chem* **280**:22165–22171.
- Tschammer N, Bollinger S, Kenakin T, and Gmeiner P (2011) Histidine 6.55 is a major determinant of ligand-biased signaling in dopamine D2L receptor. *Mol Pharmacol* **79**:575–585.
- Warne T, Moukhametzyanov R, Baker JG, Nehmé R, Edwards PC, Leslie AG, Schertler GF, and Tate CG (2011) The structural basis for agonist and partial agonist action on a β (1)-adrenergic receptor. *Nature* **469**:241–244.
- Wieland K, Zuurmond HM, Krasel C, IJzerman AP, and Lohse MJ (1996) Involvement of Asp-293 in stereospecific agonist recognition and in activation of the beta 2-adrenergic receptor. *Proc Natl Acad Sci USA* **93**:9276–9281.
- Xu F, Wu H, Katritch V, Han GW, Jacobson KA, Gao ZG, Cherezov V, and Stevens RC (2011) Structure of an agonist-bound human A2A adenosine receptor. *Science* **332**:322–327.

Address correspondence to: J. Robert Lane, Drug Discovery Biology, Monash Institute of Pharmaceutical Sciences, Monash University, 381 Royal Parade, 3052 Parkville, Australia. E-mail: rob.lane@monash.edu